Dynamics and Morphology in Nanostructured Thermoset Network/Block Copolymer Blends during Network Formation

Jovan Mijovic,* Mingzhao Shen, and Jo Wing Sy

Department of Chemical Engineering and Chemistry, Herman F. Mark Polymer Research Institute, Polytechnic University, Six Metrotech Center, Brooklyn, New York 11201

Iñaki Mondragon

Department of Chemical and Environmental Engineering, Universidad del Pais Vasco/Euskal Herriko Unibertsitatea, Avenida Felipe IV, 1-B, San Sebastian-Donostia, 20011, Spain

Received November 8, 1999; Revised Manuscript Received March 10, 2000

ABSTRACT: Molecular dynamics and morphology in the blends of a network-forming reactive polymer and an amphiphilic block copolymer were examined as a function of the advancement of chemical reactions. In the blends containing a triblock copolymer, both microscopic (domains of the order of micrometers) and nanoscopic (domains of the order of nanometers) phase separations were observed during network formation. Interestingly, only nanoscopic phase separation was found in the blends containing a diblock copolymer. The shape and the origin of these nanoscopic features were investigated by atomic force microscopy and were found to be a function of blend composition. A concept was advanced of the three-phase nanostructured morphology that begins to form with self-assembly of one block and continues to develop during network formation in the postassembly stage. The changes in relaxation dynamics that accompany network formation were monitored by broad-band dielectric relaxation spectroscopy (DRS) and were shown to represent a signature of the morphological state of the blend. The ability of DRS to identify and deconvolute various relaxation processes during network formation and phase separation is noteworthy and should be exploited as means of monitoring and controlling the development of nanostructured morphology in these complex systems.

Introduction

There is a considerable current interest among scientists and engineers in the design (or engineering) of *materials structures for desired properties and functional purposes*. A number of such *made to measure* materials have been contemplated, and some have emerged of late; an excellent account of the art of making these materials is given in the recent book by Ball, an associate editor for the journal *Nature*.[1] The key point here is that the desired properties and functions are arrived at *not* by manipulating the structure at atomic or molecular level, where the existing base of knowledge predominately lies, *but* by designing larger, nanoscopic building blocks, made of complex fluids (e.g., block copolymers, ion-containing polymers, polymer networks) and often of controlled shape (e.g., micellae, dendrimers, stars, combs, disks, columns, helices). The quest for such made to measure materials, which are bound to add a new dimension to the available range of properties and functions in polymers and other materials, is sure to play an increasingly prominent role in research and development worldwide as we enter the new millenium. The challenge, as we see it, is to revisit the conventional processing−structure−property correlations and develop new principles for creating structures of controlled length scales that would result in novel materials with distinct (and unusual) properties.

Various routes leading to these new nanostructured materials have been suggested (e.g., refs 2−8): the work described herein is aimed toward understanding the principles that underlie the development of controlled nanostructure in one such generic group of materials—those composed of an amphiphilic block copolymer and a network-forming polymer matrix. We have selected a representative system from that group of materials and have conducted a study in order to verify the feasibility of the proposed concept. The selected copolymers were diblocks and triblocks of poly(ethylene oxide), PEO, and poly(propylene oxide), PPO. PEO−PPO−PEO triblocks, in particular, were the focus of a number of recent studies because of their uses as emulsifiers, stabilizers, separation media, and drug delivery systems. The majority of those studies were performed on triblocks in solution, and a number of experimental techniques, such as static and dynamic light scattering, small-angle neutron scattering, and small-angle X-ray scattering, were employed to elucidate the effect of molecular weight and composition on the phase morphology.[9−12] Information on the dynamics of PEO−PPO−PEO triblocks in the bulk is scarce. The only published report (known to us) on the preparation of *ordered nanostructures* from a two-component mixture of a network-forming thermoset and a diblock copolymer is an excellent recent communication by Hillmyer et al.[13] These authors prepared two amphiphilic block copolymers, poly(ethylene oxide)-*block*-poly(ethylethylene) (PEO−PEE) and poly(ethylene oxide)-*block*-poly(ethylene-*alt*-propylene) (PEO−PEP), and studied their mixtures with a network-forming formulation composed of a diglycidyl ether of bisphenol A (DGEBA) epoxy resin and an aromatic amine. The cured material was characterized by an ordered core−shell nanoscopic morphology, and a TEM micrograph and SANS data were presented as evidence. The findings reported by Hillmyer and his

* To whom correspondence should be addressed. E-mail jmijovic@poly.edu.

10.1021/ma991894e CCC: $19.00 © 2000 American Chemical Society
Published on Web 06/10/2000

colleagues have provided us with an incentive to take a broader look at the chemical and physical changes that underlie the formation of these intriguing materials. In this study we describe our initial experimental attempts to track the development of nanoscopic morphology during network formation and its relation to dipole dynamics in these complex systems. A final comment: we are fully aware of, but have not cited here, a large body of literature on the subject of toughening of thermosets by rubber and high-T_g thermoplastics. The scope, the length scales, and the methodology described in this article are amply different to justify a separate consideration.

Objectives. The principal objective of this research is to monitor and describe the changes in morphology and dynamics in thermoset network/block copolymer blends during network formation.

Experimental Section

Materials. Two different systems were investigated in this study. Both systems were composed of the same network-forming formulation and a different copolymer, a diblock in one case and a triblock in the other. The diblock copolymer was poly(ethylene glycol-*co*-propylene glycol) (PEO−PPO), with average M_n = 12 000 g/mol and 70 wt % ethylene glycol. The triblock copolymer was poly(ethylene glycol)-*block*-poly(propylene glycol)-*block*-poly(ethylene glycol) (PEO−PPO−PEO), with average M_n = 4400 g/mol and 30 wt % ethylene glycol. Homopolymers were also investigated as a reference: PEO with average M_n = 8000 g/mol and PPO with average M_n = 3000 g/mol. The network-forming component was an epoxy−amine formulation. The epoxy resin was a diglycidyl ether of bisphenol A (DGEBA) with average M_n = 374 g/mol. Block copolymers, homopolymers, and the epoxy resin were obtained from Aldrich Chemical Co. Inc. The curing agent was methylenedianiline (MDA), Ciba-Geigy's HY-205, with an amine hydrogen equivalent weight of 49.5 g. The stoichiometric ratio of epoxy group to amine hydrogen was used in all formulations.

Throughout the paper, the first and the second number in each blend composition denote weight percent of the epoxy resin (DGEBA) and the copolymer (PEO−PPO or PEO−PPO−PEO), respectively. The ratio of network-forming formulation to copolymer in the blend was varied, though most results were obtained for 50/50 blends. All blends were mixed until homogeneous before testing.

Techniques. The principal experimental tool that we have used is broad-band dielectric relaxation spectroscopy (DRS). Of the experimental techniques available for the study of relaxation processes in polymeric and molecular glass formers, DRS is rapidly becoming a dominant tool.[14,15] Its great potential derives from an unparalleled frequency range available (12−14 decades) that enables one to probe molecular dynamics of condensed matter in various phases and at different temperatures: from amorphous liquids to an amorphous or crystalline glass; from high temperature, where the dipole relaxation times are of the order of tens of picoseconds, through the vitrification process where relaxation times in the glassy state reach tens to hundredths of seconds. A more detailed description of our experimental facility for dielectric measurements is given elsewhere,[16,17] and several excellent reviews of experimental methodology for dielectric measurements were recently published.[18−20] However, briefly, we have used a Solarton 1260 impedance gain phase analyzer (10 μHz−32 MHz) with broad-band dielectric converter (Novocontrol GmBh), a Hewlett-Packard (HP) 4284 A precision LCR meter (20 Hz−1 MHz), a Hewlett-Packard 4291 A RF impedance analyzer (1 MHz−1.8 GHz), and a Hewlett-Packard 8752A network analyzer (300 kHz−1.3 GHz). All instruments are interfaced to computers via IEEE 488.2 and are equipped with heating/cooling capabilities, including Novocontrol's Novocool system. A variety of sample cells were employed, including parallel plates, high-precision extension airlines, cells for the simultaneous dielectric/remote fiber-optic FTIR tests, etc. Supporting evidence was obtained from Fourier transform infrared (FTIR) spectroscopy, using Nicolet Instrument's Magna 750 spectrometer as described elsewhere,[21] differential scanning calorimetry (DSC), using TA instrument DSC model 2920 at a heating rate of 10 °C/min, optical microscopy (OM) using a Nikon HFX-II optical microscope, and atomic force microscopy (AFM), using Digital Instrument's model Nano-Scope IIIa.

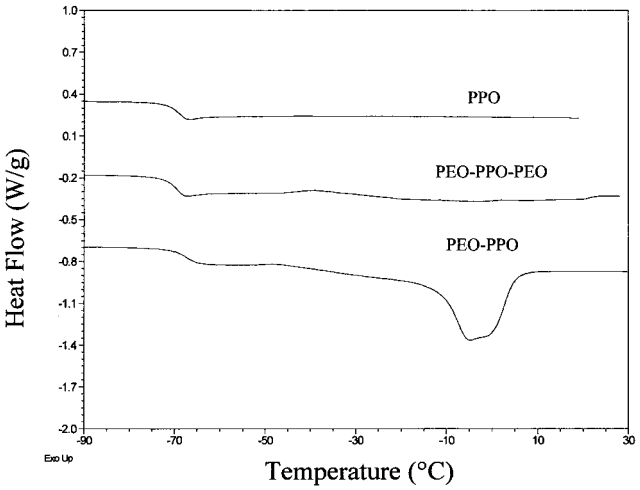

Figure 1. DSC thermograms of PPO, PEO−PPO, and PEO−PPO−PEO.

Results and Discussion

Thermal Characteristics and Dynamics of Individual Components and Blends Prior to Chemical Reaction. We begin with a recap of the principal thermal and dynamics features of the individual components of our systems and their mixtures (blends) prior to the onset of chemical reactions that led to network formation. The characteristic thermal transitions are described first. PEO is a crystalline homopolymer with a melting point (T_m) = 62 °C and a maximum attainable degree of crystallinity in excess of 80%. PPO is an amorphous homopolymer with a T_g = −69 °C. The addition of PPO to PEO (in a copolymer) hinders crystallization and reduces the melting point. The PEO−PPO diblock used in this study had a T_g = −68 °C, a broad T_m centered around −4 °C, and an estimated (from the heat of fusion) degree of crystallinity of 26%. The PEO−PPO−PEO triblock had a T_g = −69 °C, a very broad and weak melting endotherm between −20 and 20 °C, and an estimated degree of crystallinity of 13%. The corresponding DSC thermograms are shown in Figure 1. DGEBA can be easily supercooled to an amorphous glass with a T_g = −15 °C. The addition of DGEBA to a block copolymer suppresses crystallization and raises its T_g; for example, 80/20 and 50/50 DGEBA/PEO−PPO blends have T_g's of −30 and −45 °C, respectively, while 80/20 and 50/50 DGEBA/PEO−PPO−PEO blends have T_g's of −20 and −49 °C, respectively. It is important to note that all blends were initially miscible as judged by a single DSC T_g.

DRS results are described next. The measured dielectric response was quantified in terms of the relaxation time, map, strength, and spectrum, all of which are effective tools for the study of polymer dynamics. However, we shall highlight only the principal findings throughout the text. Figure 2 shows dielectric loss of PPO in the frequency domain (over 10 decades) with

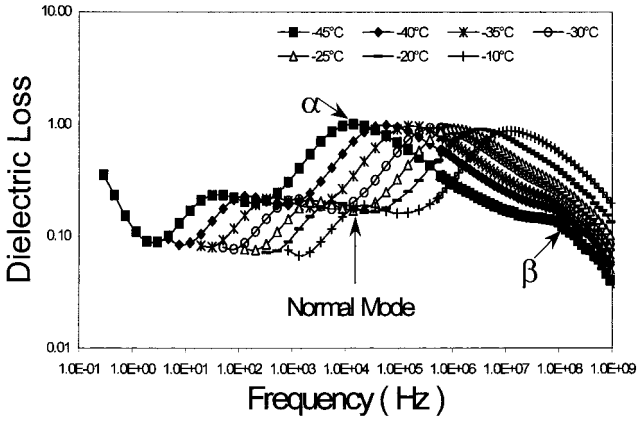

Figure 2. Dielectric loss of PPO in the frequency domain with temperature as a parameter.

temperature as a parameter. Three relaxation processes are observed in the order of increasing frequency: the α* process, due to normal mode relaxations; the α process, caused by segmental motions; and the β process, associated with the localized motions. The intensity of the α process in the crystalline PEO is much lower.

The dynamics of PEO−PPO diblock copolymer were studied next. Samples were rendered amorphous by quenching to low temperature and then swept. Three relaxation processes were observed in the order of increasing frequency: the α process, due to segmental motions, and two localized β processes, the slower one associated with PEO and the faster one with PPO. Figure 3 shows dielectric loss of PEO−PPO in the frequency domain at a series of gradually increasing temperatures. The observed decrease in the intensity of α relaxation between approximately −68 and −61 °C is caused by the onset of crystallization with increasing temperature. The two β processe are readily seen at low temperature (see arrows in Figure 3b). For example, at −76 °C, the faster process is centered around 30 kHz and the slower process around 30 Hz. Careful inspection of this figure reveals how a decrease in temperature from −72 to −107 °C causes these two β processes to evolve from the high-frequency (fast) end of the α process into two separate processes. Localized motions observed in Figure 3b are referred to as β_{PEO} (lower frequency) and β_{PPO} (higher frequency) relaxation. The identification of the origin of these two β processes in the copolymer was based on the comparison with DRS results for PEO and PPO homopolymers. Both β processes are Arrhenius, with E_a of 53.7 and 34.8 kJ/mol, respectively. DRS results for the PEO−PPO−PEO triblock also reveal three relaxation processes: the α process and two β processes.

Three relaxation processes were also observed in the dielectric spectrum of DGEBA shown in Figure 4. Two of these relaxations have been reported earlier:[22−25] a fast β process (Goldstein−Johari) due to the localized motions within the epoxide group and a slower α process attributed to segmental motions of the terminal epoxy groups on glycidyl moieties. Excellent fits of the α process to the Vogel−Fulcher−Tammann (VFT) function were obtained in accordance with the recently described procedure.[26] The third relaxation, termed β*, is located between α and β relaxations and, to the best of our knowledge, has never been reported *in the frequency domain* prior to this study. Its origin is probably in the local motions of the $-O-CH_2-CHOH-CH_2-$ moiety. Both β and β* relaxations are Arrhenius,

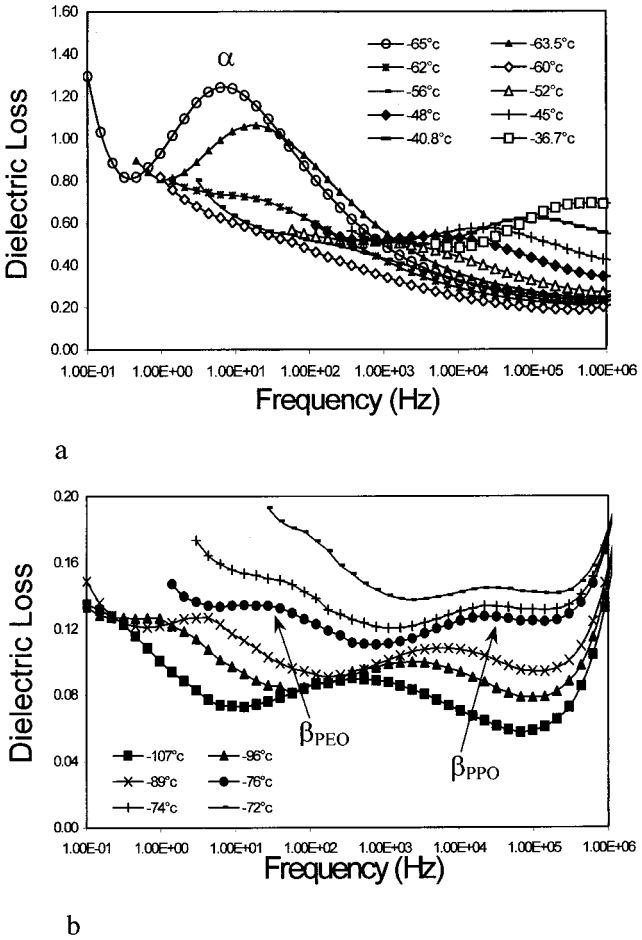

Figure 3. Dielectric loss of PEO−PPO diblock copolymer in the frequency domain with temperature as a parameter: (a) between −37 and −65 °C; (b) between −72 and −107 °C.

with activation energy (E_a) of 39.2 and 25.3 kJ/mol, respectively. Two relaxations, α and β, were also observed in MDA. The β process is Arrhenius with E_a = 42 kJ/mol. A composite relaxation map for all individual components is plotted in Figure 5.

The dynamics of blends of DGEBA and block copolymers should differ from those of the individual components, and that question was addressed next. We find that DGEBA/PEO−PPO blends of various composition have three relaxation processes: one α relaxation and two β relaxations. This is exemplified in Figure 6 that contains dielectric loss in the frequency domain for 80/20 blend with temperature as a parameter. The α process is associated with combined cooperative segmental motions of DGEBA and PEO−PPO in the blend. Fits to VFT, Havriliak−Negamy (HN),[27] and Kohlrausch−Williams−Watts (KWW)[28] functions were generated. Blending causes the broadening of the relaxation spectrum; the KWW β parameter (stretching exponent) of 0.33 is lower than that of either individual component (0.48 for DGEBA; 0.36 for PEO−PPO). This phenomenon could be attributed to an increase in intermolecular cooperativity and the increased influence of high-frequency secondary relaxation processes, although broadening of the relaxation spectrum may also originate from the concentration fluctuation that produces dynamic heterogeneities in multicomponent systems.

The two local processes are termed, in the order of increasing frequency, β_{PEO} (loss peak centered around 20 Hz at −80 °C in Figure 6b) and β_{PPO} (loss peak

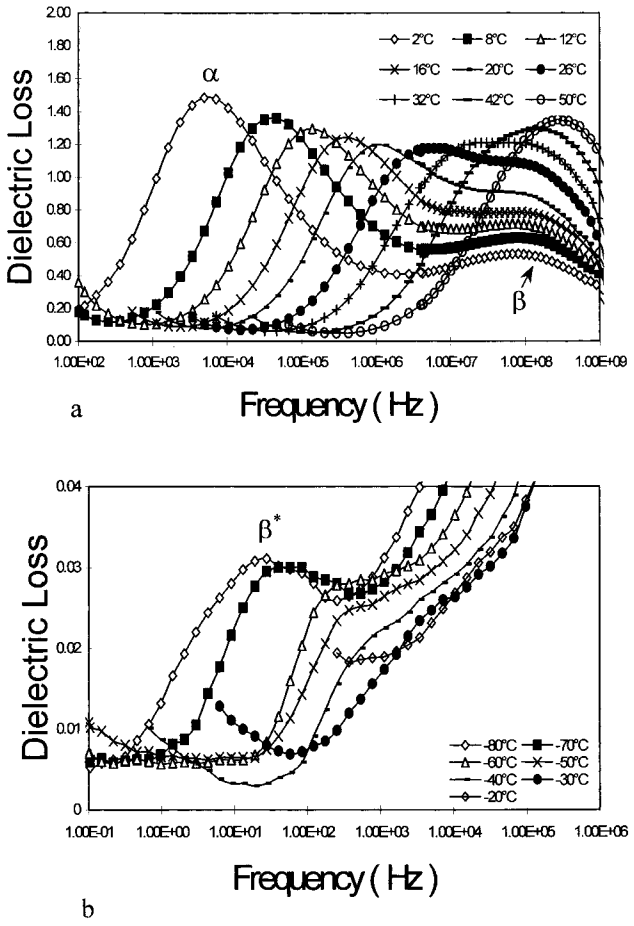

Figure 4. Dielectric loss of DGEBA in the frequency domain with temperature as a parameter: (a) between 2 and 50 °C; (b) between −30 and −70 °C.

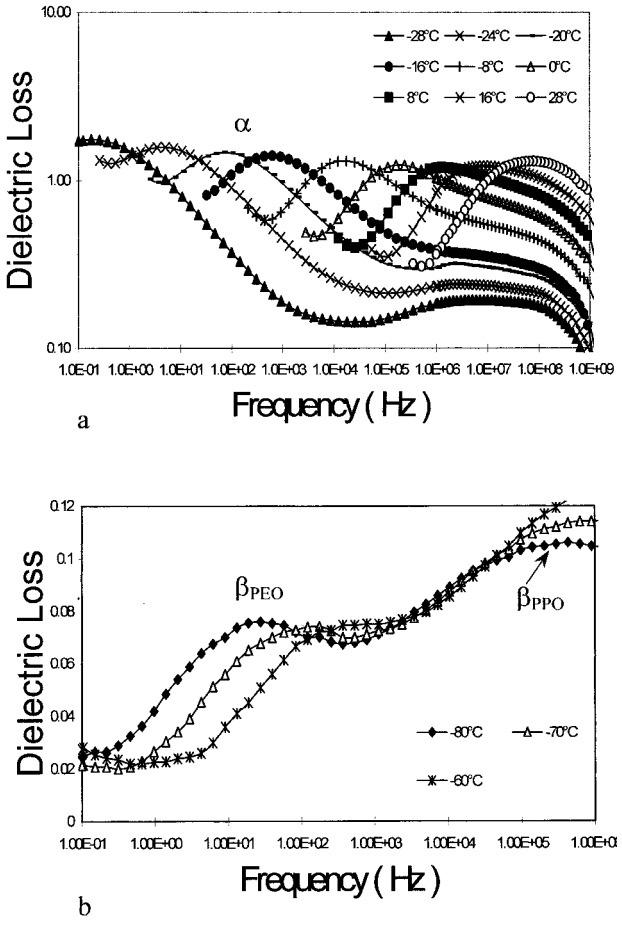

Figure 6. Dielectric loss of 80/20 DGEBA/PEO−PPO blend in the frequency domain with temperature as a parameter: (a) between −28 and +28 °C; (b) between −60 and −80 °C.

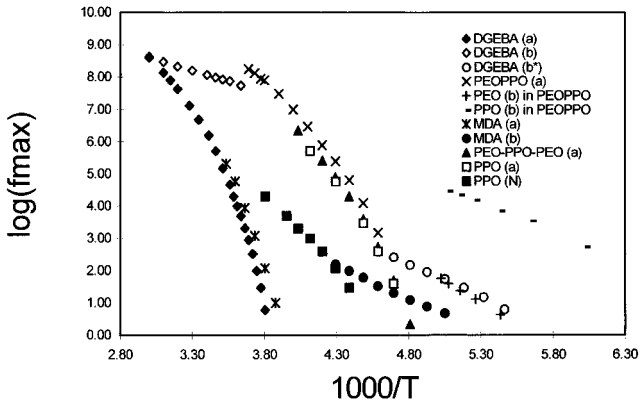

Figure 5. Frequency at maximum dielectric loss of α and β relaxations for individual components (a, b, b*, and N represent α, β, β*, and normal mode process, respectively).

centered around 400 kHz at −80 °C in Figure 6b). The general features of relaxation processes in DGEBA/triblock and DGEBA/diblock blends are similar, and we shall omit further details.

Chemical and Physical Changes in Blends during Network Formation. The progress of chemical reactions during cure in DGEBA−MDA/copolymer blends was first followed by remote fiber-optic near-infrared (NIR) spectroscopy. NIR spectra were generated at various time intervals during cure, and the extent of reaction was calculated from the areas of epoxy and reference peaks using a well-documented procedure.[21] Information about the rheological changes during cure was obtained from the measurements of steady shear viscosity. At the conditions of this study, the principal goal of the rheological measurements was to determine the gel point. Extent of reaction and viscosity are shown as a function of reaction time for DGEBA−MDA/triblock and DGEBA-MDA/diblock blend in parts a and b of Figure 7, respectively. Thermal (DSC), morphological (OM, AFM), and dynamics (DRS) results were generated at many intervals during cure (network formation) by quenching the reaction and examining the sample over the temperature range where no further reactions took place. An example of the DSC data is shown in Figure 8, which contains thermograms of 50/50 DGEBA−MDA/PEO−PPO−PEO blend taken at various times (in minutes) during cure at 120 °C. The initial mixture (0 min) has a single T_g at ca. −41 °C. During the first 45 min of cure the T_g broadens and shifts slightly to a higher temperature. Phase separation starts between 45 and 60 min and is accompanied by the emergence of two transitions: the lower one related mostly to the block copolymer and the higher one associated primarily with the DGEBA−MDA network. Note that the onset of phase separation (between 45 and 60 min) occurs at approximately 31% conversion, considerably before the gel point (located at 80 min from viscosity measurements). With further cure, the lower T_g reaches that of the copolymer, while the higher T_g increases gradually as the network continues to grow. It is interesting to note that the phase separation persists on a smaller scale after gelation (compare traces at 90, 120, and 180 min). The crystallization of the copolymer (PEO block)

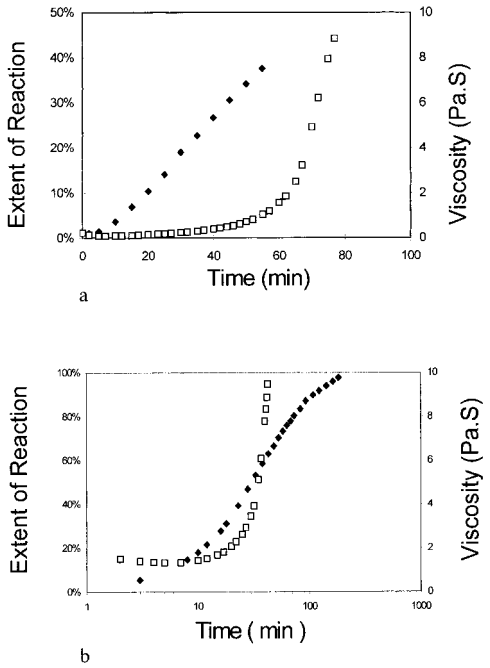

Figure 7. Extent of reaction (left ordinate) and steady-shear viscosity (right ordinate) as a function of reaction time for (a) 50/50 DGEBA−MDA/PEO−PPO−PEO blend at 120 °C and (b) 50/50 DGEBA−MDA/PEO−PPO blend at 150 °C.

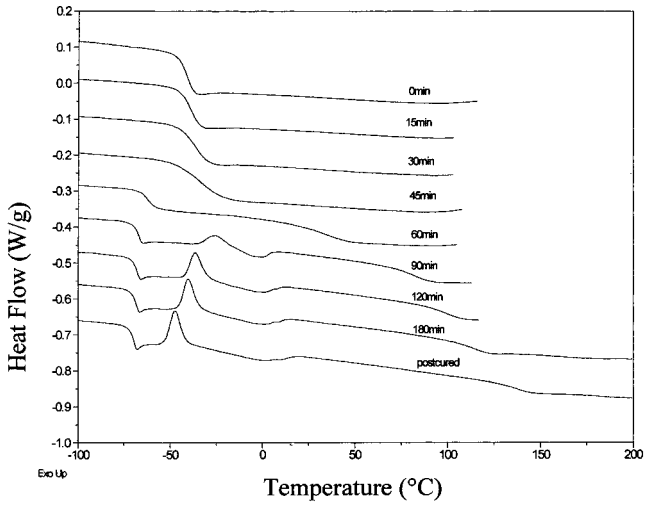

Figure 8. DSC thermograms of 50/50 DGEBA−MDA/PEO−PPO−PEO blend at various times during reaction at 120 °C.

is first detected after 90 min; the crystallization exotherm is followed by a broad melting. The continuing separation of the copolymer from the growing network during cure results in an increased mobility of the PEO blocks, and that, in turn, causes the observed shift of the onset of crystallization to lower temperature. A somewhat different result was obtained for blends containing diblock copolymer. The principal findings can be surmised from Figure 9, which contains data for the 50/50 DGEBA−MDA/PEO−PPO blend. The T_g broadens, shifts ever so slightly to higher temperature, and flattens out considerably. Phase separation that was manifested by the emergence of two distinct T_g's in the triblock-containing blends (Figure 8) is largely absent here. Enlarged DSC thermograms of samples cured between 30 and 120 min show a very broad endothermic transition between 50 and 100 °C, but one would be hard pressed to define a single T_g there. The upper

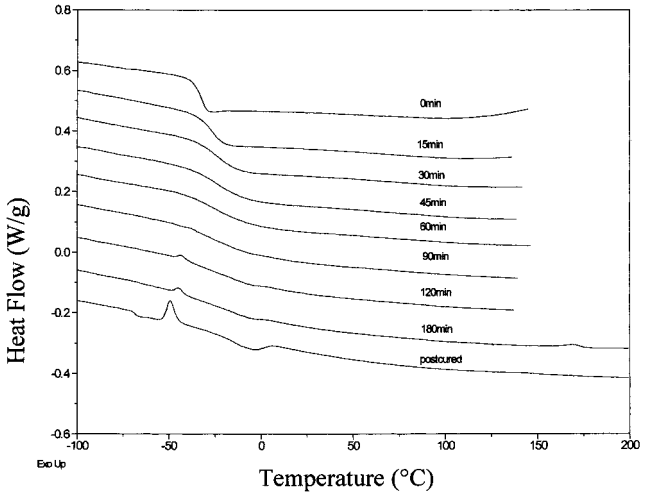

Figure 9. DSC thermograms of 50/50 DGEBA−MDA/PEO−PPO blend at various times during reaction at 150 °C.

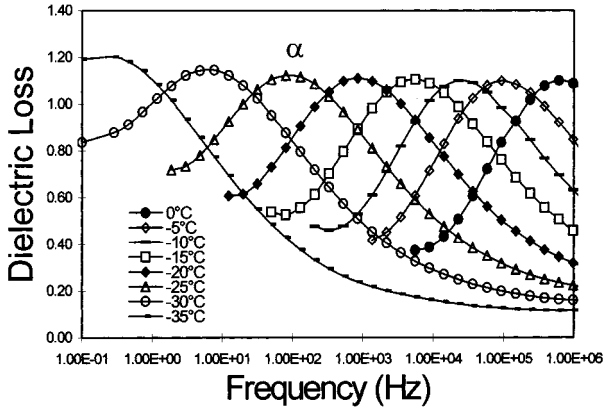

Figure 10. Dielectric loss of 50/50 DGEBA−MDA/PEO−PPO−PEO blend in the frequency domain before cure with temperature as a parameter: (a) between 0 and −35 °C; (b) between −50 and −60 °C.

temperature limit in the DSC thermograms of the partially cured samples was imposed to avoid the continuation of chemical reactions. After 180 min of cure we observe two small exotherms, at low temperature due to crystallization of PEO and at high temperature due to additional chemical reactions, but we could not detect a distinct T_g of the cured network even after postcure. We therefore conclude that the resulting morphology on the microscopic (domains of the order of micrometers) level is best described as a continuous phase of epoxy network and block copolymer with a broad glass transition. Of course, this does not imply a priori the absence of any *nanoscopic* phase separation within the DGEBA−MDA-rich phase. Corroborating evidence for this concept was obtained from DRS and AFM and is presented below.

DRS of DGEBA−MDA/PEO−PPO−PEO Blends during Network Formation. Whether and how the changes observed by DSC affect dynamics are examined next. Dielectric loss in the frequency domain at different temperature for 50/50 DGEBA−MDA/PEO−PPO−PEO blend prior to the onset of reactions is shown in Figure 10. The α process, associated with combined segmental molecular motions in the miscible phase of DGEBA, MDA, and PEO−PPO−PEO, is prominent. This relaxation is slower than that in the blend without MDA primarily due to the addition of a higher T_g component (MDA). We now examine the DRS spectra at various

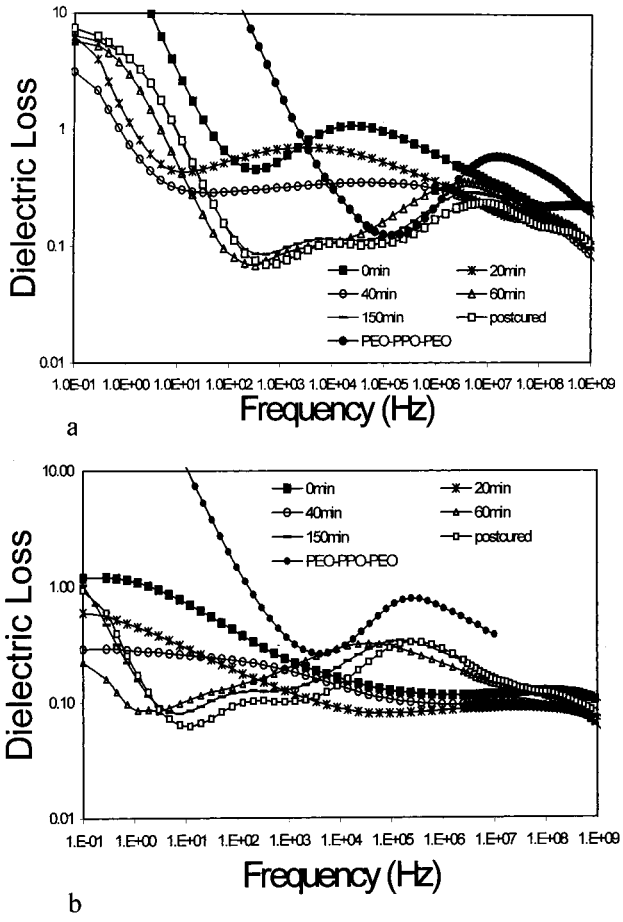

Figure 11. Dielectric loss of 50/50 DGEBA−MDA/PEO−PPO−PEO blend with reaction time at 120 °C as a parameter, measured at (a) −10 °C and (b) −35 °C. (All measurements were performed on the amorphous samples.)

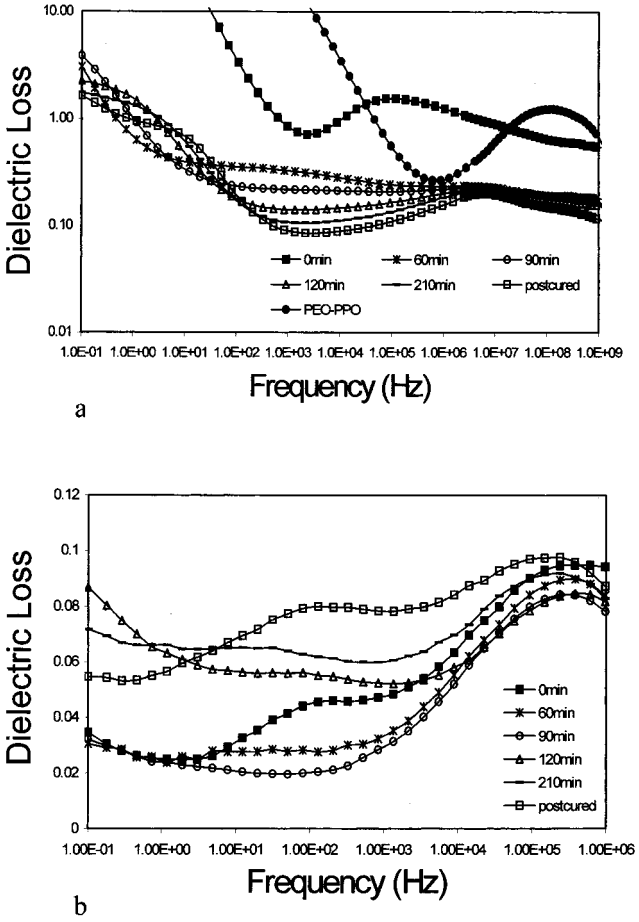

Figure 12. Dielectric loss of 50/50 DGEBA−MDA/PEO−PPO blend with reaction time at 150 °C as a parameter, measured at (a) −10 °C and (b) −56 °C. (All measurements were performed on the amorphous samples.)

intervals during cure. Figure 11 shows dielectric loss in the frequency domain with reaction time at 120 °C as a parameter. Note that the measurements were conducted at −10 °C (Figure 11a) and at −35 °C (Figure 11b). At −10 °C, the α process is initially (0% conversion) centered around 1 kHz. The overall decrease in the segmental mobility during network formation is reflected in the shift of the α process to lower frequency, clearly seen after 20 min of cure. A simultaneous decrease in the intensity of the α process also reflects the broadening of the spectrum and the depletion of more polar dipoles. Further cure causes additional broadening and flattening of the loss spectrum. Consequently, meaningful fits to HN and KWW functions were possible only during the early stages of network formation. For example, the KWW parameter β decreases from 0.32 to about 0.25 during the first 15% of cure. Although this trend is in agreement with the previously reported results for neat epoxy networks,[23,26] the KWW β parameters at comparable degrees of crosslinking are higher in neat epoxies than in the blends with triblock copolymer, suggesting a broader distribution of domains in the latter group. The effect of phase separation is evident in the loss spectrum taken at 60 min; the α process associated with the curing network shifts below 0.1 Hz, and two more processes emerge in the frequency window of Figure 11. These two processes, more clearly seen in Figure 11b, are associated (in the increasing order of frequency) with normal mode relaxation in PPO and segmental relaxation in the triblock. Both peaks shift to *higher frequency* with further cure as a result of continuing phase separation. The assignment of the peak at lower frequency to normal mode relaxations in PPO was further supported by contrasting Figure 11 with the dielectric spectra of neat PPO, PPO blocks in the triblock, and postcured DGEBA−MDA/PPO blend: the location of the maximum loss for normal mode in all these samples is identical. Also, the frequency location of the maximum loss due to segmental relaxation in the PEO−PPO−PEO phase of the fully cured blend is identical to that in the neat triblock (see trace in Figure 11). Finally, a new low-frequency process emerges during network formation, with the high-frequency tail of its loss spectrum becoming clearly visible (see Figure 11a) after approximately 40 min of cure. The large magnitude of this new process suggests that its origin could not be related to the dipole moment of any single blend component. Considering that the emergence of this process coincides with the onset of phase separation, it is likely that its origin lies in the interfacial (Maxwell−Sillars) polarization.

DRS of DGEBA−MDA/PEO−PPO Blends during Network Formation. Dielectric loss in the frequency domain of 50/50 DGEBA−MDA/PEO−PPO blend with reaction time at 150 °C as a parameter is depicted in Figure 12. Two sets of measurements are shown: at −10 °C (Figure 12a) and at −56 °C (Figure 12b). The dielectric spectra also reflect the morphological change during network formation. The α process, which is initially (0% conversion) centered at 100 kHz at −10

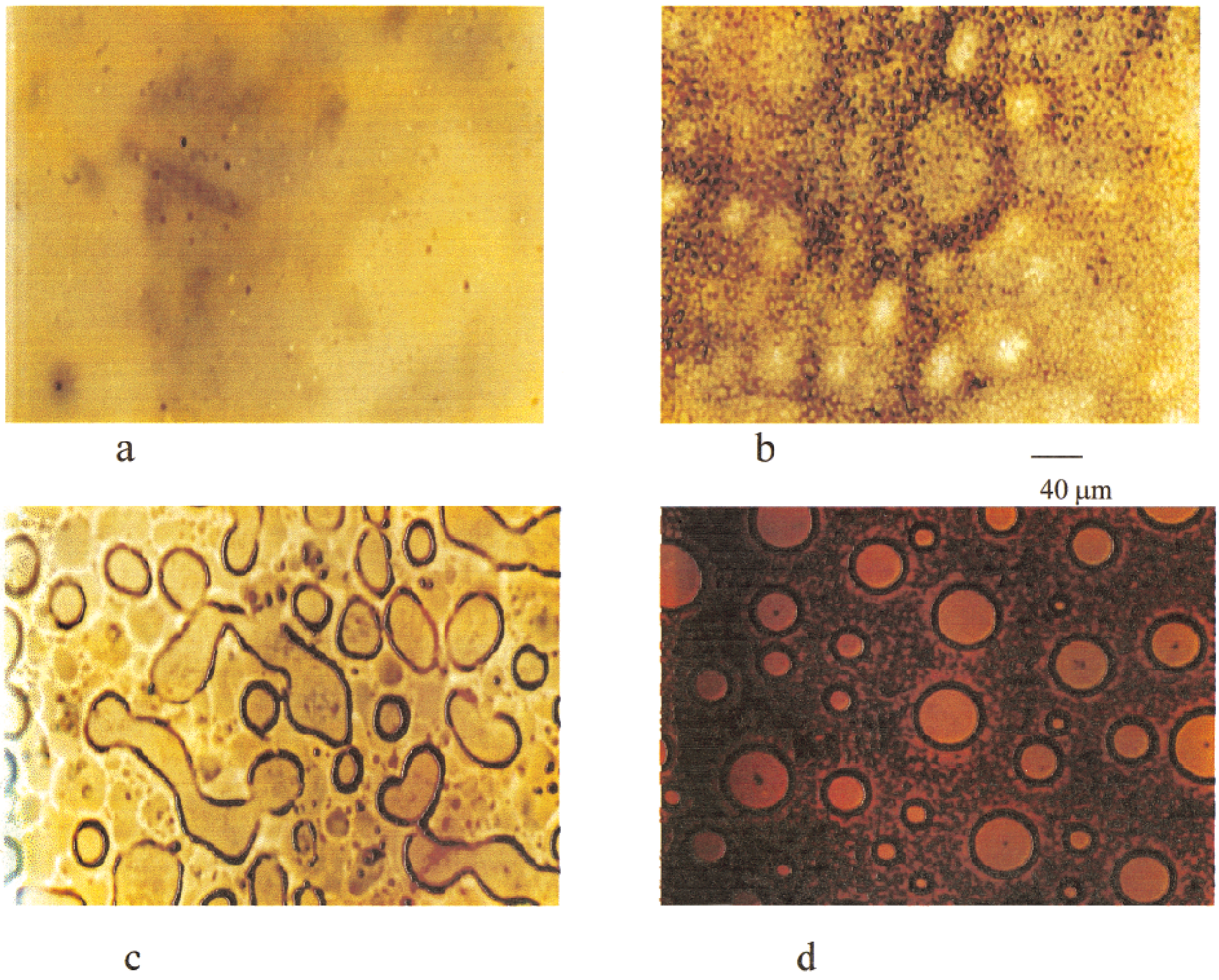

Figure 13. Optical micrographs of 50/50 DGEBA−MDA/PEO−PPO−PEO blend at various times during cure at 120 °C: (a) 27 min, (b) 52 min, (c) 125 min, and (d) 80/20 DGEBA−MDA/PEO−PPO−PEO blend after 35 min.

°C (Figure 12a), shifts to lower frequency and becomes broader during the first 90 min of cure. Fits to the VFT function were generated up to approximately 50% cure. In that interval, the average relaxation time increases by 2 decades and the dielectric strength decreases by about 20%. The KWW β parameter remained practically constant ($\beta = 0.32$) until about 50% conversion (in stark contrast with the triblock-containing blends), at which point we obtained the best fit value of $\beta = 0.28$. A constant KWW β indicates that the distribution of domains does not appreciably change in this conversion range. In a recent study of the dynamics of DGEBA−DETA formulation during cure, it was found that a KWW β parameter of 0.28 gave the best fit in the conversion range from 30 to 56%.[26] Low-temperature spectra (Figure 12b) show the emergence (after 90 min) of a new peak at about 100 Hz at −56 °C. We believe this peak is associated with the segmental motions within the diblock-rich phase (corresponding to the low-T_g phase observed by DSC) for the following reasons. First, this process is initially absent, and it develops as the cross-linking progresses. The shoulder located at a similar frequency at 0 min is due to the β* process in DGEBA, and it disappears during cure. The new process appears and starts to grow after 90 min at a location that is almost identical to that of the α process in the neat diblock at the same temperature. A question may arise as to the low intensity of this peak and its apparent resemblance to a β process, but that can be explained. For example, we compared the low-T_g ΔC_p for the neat diblock and the postcured blend (normalized by the diblock content) and found that ΔC_p was only $^1/_3$ that of the neat diblock. A plausible explanation is that only a part of the diblock resides in the low-T_g phase, which would account for the low intensity of the new peak. Furthermore, at −56 °C, some PEO segments have crystallized, and the low peak intensity reflects both a decrease in the amount of the amorphous phase and an increase in the constraints introduced by the crystalline phase. Supporting evidence was obtained for DRS and DSC measurements of quenched and slowly cooled postcured blends, which were designed to amplify the effect of crystallization. Indeed, the intensity of this new peak was found to decrease due to crystallization. And finally, the temperature dependence of this new relaxation was typical of an α, not a β, process. On the basis of these observations, we conclude that this new emerging peak is due to the α process associated with segmental relaxations in the low-T_g phase.

Morphology of DGEBA−MDA/PEO−PPO−PEO Blends during Network Formation. Morphological developments during cure were studied by optical microscopy (OM) and atomic force microscopy (AFM) and are described next. To avoid any possible confusion, we stress that the terms *microscopic* and *nanoscopic* are used here to describe the presence of domains of the

order of *micrometers* and *nanometers*, respectively. The triblock-containing blend is initially homogeneous and transparent under OM. Gradually, however, microscopic phase separation sets in and the blend turns opaque. The gradual change in the morphology during network formation in 50/50 DGEBA−MDA/PEO−PPO−PEO blend is described in the optical micrographs of Figure 13. After approximately 27 min at 120 °C we observe the sudden emergence of a number of small, roughly spherical entities throughout the mixture (Figure 13a). They typically grow in size, and some collide and collapse to form larger entities (Figure 13b). Postcured samples are characterized by the presence of "islands" (Figure 13c). Interestingly, the morphological pattern observed during network formation is a function of blend composition. For example, 80/20 DGEBA−MDA/PEO−PPO−PEO blend, rich in the network-forming component, is characterized by the sudden appearance of almost perfectly spherical entities that change little in shape and number with further cure (Figure 13). Viewed under the optical microscope, the formation of this morphology (Figure 13d) appears to occur by nucleation and growth, and the spherical occlusions seem to contain the block copolymer. Further attempts to study the mechanism of phase separation by OM were not made in this study but are currently underway in our laboratories. The results of AFM investigation were most revealing in that they confirmed the existence of phase separation on a smaller scale as well. Figure 14a shows a higher magnification image of the morphology of a fully cured 50/50 DGEBA−MDA/PEO−PPO−PEO blend, which was taken in the area between inclusions shown in Figure 13d. Morphological features of greatly varying size (some of the order of hundreds of nanometers) and shape are observed. We shall defer the interpretation of the origin of these nanoscopic regions until the end of next section.

Morphology of DGEBA−MDA/PEO−PPO Blends during Network Formation. In comparison to the above-described findings, there was one major difference in the morphology of diblock-containing blends during cure. Viewed under OM, these blends remain transparent throughout cure, suggesting the absence of microscopic phase separation. But the AFM micrographs of fully cured DGEBA−MDA/PEO−PPO blends show nanoscopic phase separation for various compositions (80/20, Figure 14b; 50/50, Figure 14c). The size, shape, and uniformity of the nanoscopic features (see Figure 14b,c) are distinctly different from those observed in the triblock-containing blends (see Figure 14a). The average size in the diblock-containing blends is of the order of 10−30 nm. The shape is very regular and uniform, particularly in the 80/20 blend (Figure 14b) where the characteristic features appear predominantly circular (spherical in 3-D). The emerging three-phase pattern, characterized by features of the order of 10−30 nm, resemble the TEM micrograph obtained by Hillmyer.[13] Therefore, it seems reasonable to conclude that the resulting morphology can be described with some confidence, while recognizing that much remains to be learned about the origin and formation of each nanophase. A conceptual view of how an ordered nanoscopic morphology forms in our systems is offered in the schematic of the gradual development of an organized nanostructure during network formation, shown in Figure 15A−E (clockwise). Let us assume that the blend contains a block copolymer and that each block is

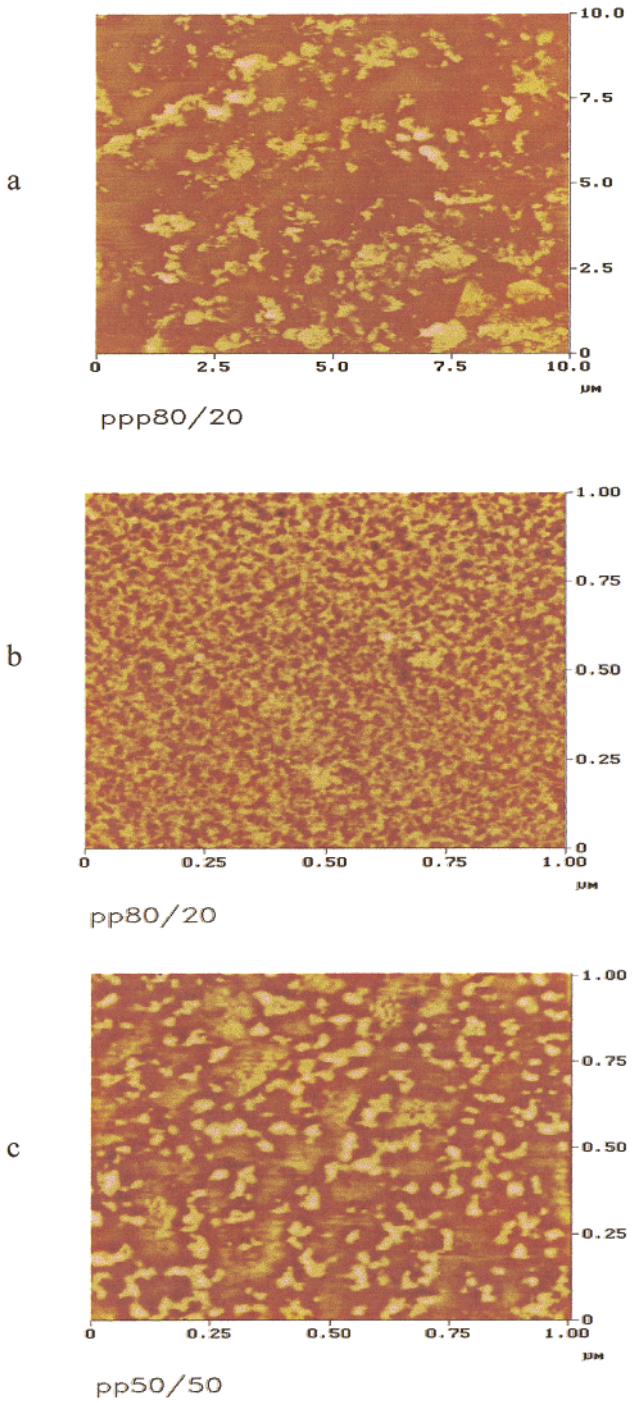

Figure 14. AFM image of fully cured (a) 80/20 DGEBA−MDA/PEO−PPO−PEO blend, (b) 80/20 DGEBA−MDA/PEO−PPO blend, and (c) 50/50 DGEBA−MDA/PEO−PPO blend.

represented by a different color, red and green. Specifically, assume that PEO−PPO block copolymer is used and that red and green are the colors of PEO and PPO segments, respectively. Reactive groups in the network-forming formulation (say, DGEBA−MDA) are represented by circles (epoxy) and squares (amine hydrogens). Figure 15A represents the instantaneous state upon mixing. Subsequently, the PPO (green) blocks self-assemble into nanoscopic entities dispersed in the miscible phase composed of PEO (red) and the epoxy−amine formulation (a negative Flory−Huggins parameter χ has been reported). This is represented by Figure 15B. Whether the inner core is composed entirely of PPO and to what extent the PPO blocks self-assemble as envi-

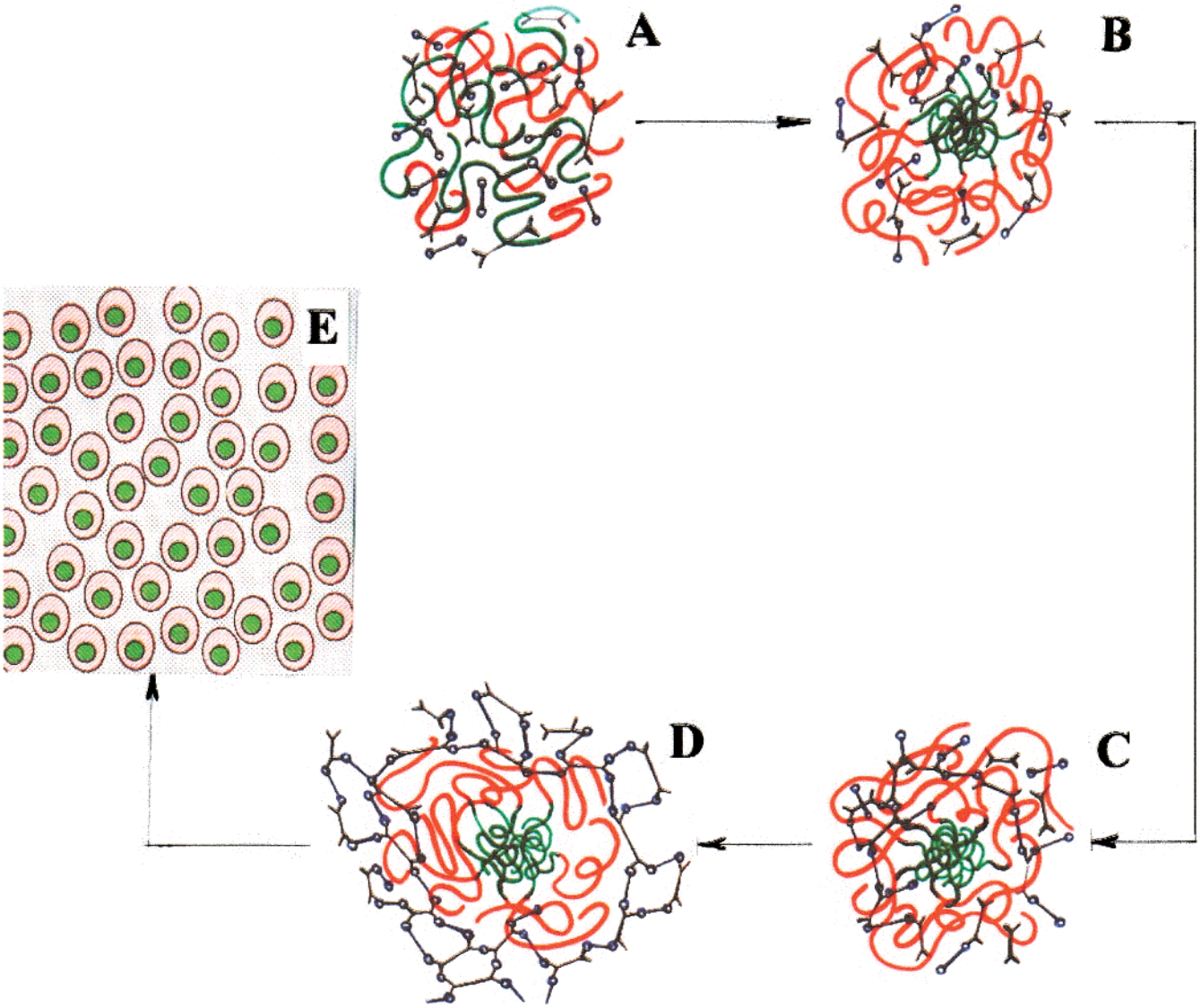

Figure 15. Schematic of the development of nanoscopic morphology in our systems.

sioned in Figure 15B is not completely clear. Nonetheless, network formation gathers speed in the postassembly stage and continues as shown in Figure 15B,C. During some "critical" stage of cure, however, PEO (red) separates out (gradually), and that gives rise to the morphology shown in Figure 15D. The surrounding nanophase (middle layer) is likely to contain PEO mixed with some partially cured DGEBA−MDA network. The outer area (third nanoscopic phase) is composed primarily of the DGEBA−MDA network. Ideally, a larger section of that sample should have a well-defined nanoscopic morphology, schematically shown in Figure 15E.

For the end, we reserve a comment regarding the challenging task of describing the formation of nanostructured morphology in thermoset network/block copolymer blends by computational modeling. The work performed in this study was predominantly experimental with some phenomenological analysis of the DRS data, and it is clear that understanding and analysis of nanostructure evolution in these complex systems, its dependence on material parameters, and its response to electrical, mechanical, and thermal stresses require quantitative modeling based on sound physical principles. Computational modeling of materials and processes poses a grand challenge in systems that exhibit nonlinear, nonequilibrium, collective dynamics coupling macromolecular degrees of freedom to transport of momentum, to externally applied fields, and to chemical reactions. A hierarchical multiscale organization of local order parameters emerges in both space and time, as evidenced by the emergence of both micro- and nanophase separated, strongly segregated domains. This precludes reliance on simplified models invoking equilibrium or steady-state conditions, Landau−Ginzburg expansions in small-order parameters and their first derivatives, and Newtonian constitutive relations. A computational model faithfully representing the entire gamut of the physics underlying the complex dynamics in our experimental systems does not exist at present, and its development is highly desirable.

Summary and Conclusions

An investigation of the morphological changes in thermoset network/copolymer blends during the advancement of chemical reactions has shown that the formation of nanostructural organization in these complex systems is feasible. In the blends containing triblock copolymers we observed phase separation during network formation on both the microscopic and nanoscopic scale. In the diblock-containing blends,

however, only nanoscopic phase separation was detected. The shape and the size of these nanoscopic features were a function of blend morphology. In fully cured 80/20 DGEBA−MDA/PEO−PPO blend, for example, a three-phase morphology was found, reminiscent of the TEM image observed by Hillmyer.[13] The likely scenario for the development of nanoscopic morphology starts with the self-assembly of one block of the amphiphilic copolymer and proceeds with a gradual separation of the other block from the growing network. An important consideration is how nanoscopic and macroscopic phase separation are affected by the presence and/or absence of entanglements in the triblock copolymer.

The demonstrated ability of DRS to track the changes in dipole dynamics during the various morphological developments in these complex systems is noteworthy. In general, we were able to observe the slowing down and broadening of the α process due to segmental molecular motions in the growing network, the emergence of normal mode relaxation in PPO blocks and segmental relaxations in PEO−PPO and PEO−PPO−PEO copolymers, and the appearance of interfacial polarization. Identification and deconvolution of various relaxation processes during network formation and phase separation by DRS appear possible and should be further explored as means for quantitative monitoring of the development of nanostructured morphology in complex systems.

In sum, our experimental findings are interesting but preliminary; a continuing systematic study of processing−morphology−property relationships in these complex systems, experimental and theoretical, is necessary to develop new principles for creating structures of controlled length scales that would result in novel materials with distinct (and unusual) properties. A systematic investigation is recommended of a series of network-forming/amphiphilic block copolymer blends selected on the basis of fundamental considerations that include, but are not limited to, molecular parameters (e.g., molecular weight, type and distribution of blocks, type and functionality of network-forming components), processing parameters (e.g., cure temperature), intensity and molecular origin of relaxations, types of dipoles present, and molecular architecture (T_g, T_m). Such investigation should be conducted in concert with computational modeling.

Acknowledgment. This material is based on work supported by the National Science Foundation under Grants DMR-9710480 and INT-9724714.

References and Notes

(1) Ball, P. *Made to Measure: New Materials for the 21st Century*; Princeton University Press: Princeton, NJ, 1998.
(2) Whitesides, G. M.; Mathais, J. P.; Seto, C. *Science* **1991**, *254*, 1312.
(3) Martin, C. R. *Science* **1994**, *266*, 1961.
(4) Firouzi, A.; et al. *Science* **1995**, *267*, 1138.
(5) Collins, P. G.; Zettl, A.; Bando, H.; Thess, A.; Smalley, R. E. *Science* **1997**, *278*, 100.
(6) A number of recent research papers on this subject were presented at and can be found in: *Proceedings of the IUPAC World Polymer Congress*, Gold Coast, Australia, July 12−17, 1998.
(7) A number of recent research papers on this subject were presented at and can be found in: *Proceedings of the Spring Meeting of the American Chemical Society*, Anaheim, CA, March 1999.
(8) Kalinina, O.; Kumacheva, E. *Macromolecules* **1999**, *32*, 4122.
(9) Chu, B.; Zhou, Z. In *Nonionic Surfactants: Polyoxyalkylene Block Copolymers*; Surfactant Science Series Vol. 60; Nace, V. M., Ed.; Marcel Dekker Inc.: New York, 1996.
(10) Alexandridis, P.; Holzwarth, J. F.; Hatton, T. A. *Macromolecules* **1994**, *27*, 2414.
(11) Noolandi, J.; Shi, A.; Linse, P. *Macromolecules* **1996**, *29*, 5907.
(12) Brown, W.; Schillen, K.; Hvidt, S. *J. Phys. Chem.* **1992**, *96*, 6038.
(13) Hillmyer, M. A.; Lipic, P. M.; Hajduk, D. A.; Almdal, K.; Bates, F. S. *J. Am. Chem. Soc.* **1997**, *119*, 2749.
(14) Williams, G. In *Keynote Lectures in Selected Topics of Polymer Science*; Riande, E., Ed.; CSIC: Madrid, Spain, 1995; Chapter 1, pp 1−40.
(15) Fitz, B.; Mijovic, J. *Macromolecules* **1999**, *32*, 3518.
(16) Fitz, B.; Andjelic, S.; Mijovic, J. *Macromolecules* **1997**, *30*, 5227.
(17) Andjelic, S.; Mijovic, J.; Bellucci, F. *J. Polym. Sci., Part B: Polym. Phys.* **1998**, *36*, 641.
(18) Williams, G. In *Dielectric Spectroscopy of Polymeric Materials*; Runt, J. P., Fitzgerald, J. J., Eds.; American Chemical Society: Washington, DC, 1997; Chapter 1, pp 3−65.
(19) Kranbuehl, D. E. In *Dielectric Spectroscopy of Polymeric Materials*; Runt, J. P., Fitzgerald, J. J., Eds.; American Chemical Society: Washington, DC, 1997; Chapter 13, pp 303−328.
(20) Kremer, F.; Arndt, M. In *Dielectric Spectroscopy of Polymeric Materials;* Runt, J. P., Fitzgerald, J. J., Eds.; American Chemical Society: Washington, DC, 1997; Chapter 15, p 423.
(21) Mijovic, J.; Andjelic, S. *Macromolecules* **1996**, *29*, 239.
(22) Pochan, J. M.; Gruber, R. J.; Pochan, D. F. *J. Polym. Sci., Polym. Phys. Ed.* **1981**, *19*, 143.
(23) Andjelic, S.; Fitz, B.; Mijovic, J. *Macromolecules* **1997**, *30*, 5239.
(24) Corezzi, S.; Capaccioli, S.; Gallone, G.; Livi, A.; Rolla, P. A. *J. Phys.: Condens. Matter* **1997**, *9*, 6199.
(25) Casalini, R.; Fioretto, D.; Livi, A.; Lucchesi, M.; Rolla, P. A. *Phys. Rev. B* **1997**, *56*, 3016.
(26) Fitz, B.; Mijovic, J. *Macromolecules* **1999**, *32*, 4134.
(27) Havriliak, S.; Negami, S. *Polymer* **1967**, *8*, 161.
(28) Williams, G.; Watts, D. C. *Trans. Faraday Soc.* **1970**, *66*, 80.

MA991894E